Nucleation of cobalt silicide islands on Si(111)-7 × 7

2006 J. Phys.: Condens. Matter 18 6987

(http://iopscience.iop.org/0953-8984/18/30/004)

INSTITUTE OF PHYSICS PUBLISHING JOURNAL OF PHYSICS: CONDENSED MATTER

J. Phys.: Condens. Matter **18** (2006) 6987–6995 doi:10.1088/0953-8984/18/30/004

Nucleation of cobalt silicide islands on Si(111)-7 × 7

M A K Zilani, Lei Liu, H Xu, Y P Feng, X-S Wang and A T S Wee[1]

Department of Physics, 2 Science Drive 3, National University of Singapore, Singapore 117542, Republic of Singapore

E-mail: phyweets@nus.edu.sg

Received 4 April 2006, in final form 20 June 2006
Published 14 July 2006
Online at stacks.iop.org/JPhysCM/18/6987

Abstract

We present a scanning tunnelling microscopy (STM) investigation of Co silicide cluster and island formation on Si(111)-(7 × 7). We identify sub-nanometre clusters, which we propose to be the precursors to Co silicide nucleation and growth. The observation of metastable phases and various domains on the surface suggest significant Si rearrangement during silicide formation. Surface diffusion of both Si and type-1 clusters plays a vital role in the nucleation of Co silicide islands. With the help of density functional theory calculations, we propose a model for the surface structure of atomically flat $CoSi_2$(111)-(2 × 2) islands.

(Some figures in this article are in colour only in the electronic version)

1. Introduction

The electronic properties of devices depend critically on the metal–semiconductor interface structure. In particular, the interaction of metals with Si has attracted much interest in the fabrication of non-volatile memories and as contacts in MOSFET device fabrication [1, 2]. Most metals react with Si at moderate temperatures, so the properties of interfaces are determined by the silicidation process. The silicide interface structures formed during deposition of a thin metal film are often different from the bulk silicide equilibrium phase. Scanning tunnelling microscopy (STM) allows localized measurements at atomic resolution, and can in principle probe atomic-scale precursors, surface structure, kinetics and the evolution of atoms, clusters and islands [3].

Due to the reactive nature of 3d ferromagnetic metals Co and Fe with Si(111)-(7 × 7), substantial rearrangements of substrate atoms occur even at room temperature (RT) [4, 5]. These systems cannot be explained by simple growth models such as the Stranski–Krastanov (S–K) growth model for Si/Ge(111) [6] or the Vollmer–Weber (V–W) growth model for

[1] Author to whom any correspondence should be addressed.

Ag/Si(111)-H [7]. Wawro *et al* observed that, when 0.33 monolayers (ML) of Fe on Si(111)-(7 × 7) was annealed at 250 °C, 'three-atom rings' were formed on the surface, and postulated that these rings are precursors to the 2 × 2 reconstructed Fe silicide islands [8]. For room-temperature (RT) deposition of Co at low coverage (∼0.016 ML) on Si(111)-(7 × 7), Bennett *et al* identified a few Si adatoms with different image contrast and proposed that the deposited Co atoms occupy near-surface interstitial sites [9]. In a separate study at 0.1 ML Co coverage annealed to 670 °C, Bennett *et al* observed ring clusters (RCs) in the Si(111)-($\sqrt{7} \times \sqrt{7}$)Co reconstruction, and postulated these as intermediate structures between clean and silicide–Si interfaces [4, 10]. Reference [3] reviews STM studies of silicides. Furthermore, Vrijmoeth *et al* and Hellman *et al* have studied Co silicide epitaxial growth on Si(111) and explained the interface and surface structure using Auger electron spectroscopy, Rutherford backscattering, transmission electron microscopy, and medium-energy ion scattering [11, 12].

In this paper, we present an STM study of the nucleation of Co silicide clusters and islands on Si(111)-(7 × 7). Based on our experimental observations, a model of the $CoSi_2$(111)-(2 × 2) surface structure is proposed, supported by density functional theory (DFT) calculations.

2. Experimental details

We performed *in situ* experiments in a multi-chamber ultra-high-vacuum (UHV) system with a base pressure of 2×10^{-10} mbar [13]. The analysis chamber is equipped with an Omicron variable temperature (VT)-STM, x-ray photoelectron spectroscopy (XPS), and low-energy electron diffraction (LEED) optics. The Si(111)-7 × 7 reconstructed surface was prepared by degassing the sample at 500 °C for several hours, and repeated flashing to 1200 °C using resistive heating, maintaining the chamber pressure below 1×10^{-9} mbar. Co was evaporated onto the surface at a deposition rate of ∼0.1 ML min^{-1} (where 1 ML = 7.83×10^{14} Co atoms cm^{-2}) from an electron-beam evaporator. STM was employed to image the topography in constant-current mode. XPS and LEED were routinely carried out to check the surface cleanliness and reconstruction.

3. Results

We deposited Co on Si(111)-7 × 7 at RT and subsequently annealed the substrate to different temperatures for different durations. Such growth processes, where the clusters are grown by post-deposition annealing, are known as solid-phase epitaxy (SPE) [14]. Figure 1(a) shows a three-dimensional (3D) STM image of a ∼0.4 monolayer (ML) Co deposited substrate after annealing at 300 °C for 3 min. Flat-top islands with atomically resolved corrugations are clearly observed. In the inter-island regions, we can resolve regions displaying the Si(111)-7 × 7 reconstruction, highlighted by the dotted ellipse. The high-resolution empty-state image of the inter-island area in figure 1(b) shows the Co-induced RCs co-existing with Si(111)-(7 × 7) (marked by dotted arrows), consistent with previous work on Ni and Co [4, 15]. In a regular array, the RCs were previously identified as Si(111)-($\sqrt{7} \times \sqrt{7}$)Co [4, 15]. Figure 1(c) shows that the corrugation period on this island is ∼7.5 ± 0.2 Å, or about 2 × a (=7.6 Å), where a = 3.8 Å is the lattice constant of unreconstructed $CoSi_2$, suggesting that the reconstruction is indeed $CoSi_2$(111)-2 × 2.

The surface in figure 1(a) was further annealed at 400 °C for 3 min, and is shown in figures 2–4. Different types of clusters and Si(111)-7 × 7 unit cells in the inter-cluster areas are observed on the surface and explained below. The clean Si(111)-7 × 7 surface area increases with higher-temperature annealing. Straight lines are drawn in figure 2 to demarcate the

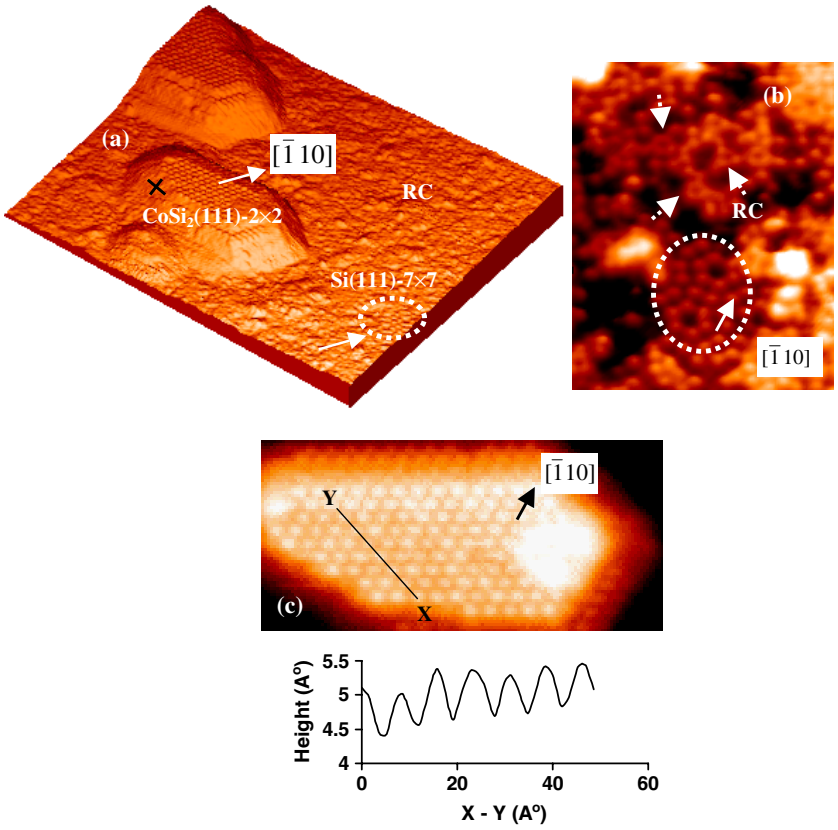

Figure 1. Empty-state STM image ($V_{tip} = -1.8$ V) of $CoSi_2$(111)-(2 × 2) islands formed after ∼0.4 ML Co deposited on Si(111)-(7 × 7) at RT is annealed at 300 °C for 3 min. (a) 3D representation; scan size = 457 × 356 Å^2. Patches of Si(111)-(7 × 7) reconstruction are shown by a dotted ellipse. The arrow is along the [$\bar{1}$10] direction separating FH and UH, joining two corner holes of 7×7; it also corresponds to one of the unit cell directions of $CoSi_2$(111)-(2×2). (b) A small portion zoomed from the inter-island areas clearly shows patches of Si(111)-(7 × 7) reconstruction and the RCs (marked by a dotted arrow). (c) STM image of a $CoSi_2$(111)-(2 × 2) island, and the line profile between two points *X* and *Y* marked on this image.

Si(111)-7 × 7 unit cells. The dotted ellipses highlight discontinuities in the Si(111)-7 × 7 unit cells due to dislocations.

By analysing a large number of similar STM images obtained under similar conditions, we categorize the observed clusters into three types by size and structure: type-1 clusters are small with diameter ∼8.9 ± 0.2 Å in filled-state STM images (figures 2 and 3). They are randomly distributed on the terraces but are observed at higher densities near type-2 clusters (figures 2 and 3). Type-2 clusters have base areas limited to between one to 14 times the 7 × 7 unit cell area. The cluster shape is arbitrary in both lateral and perpendicular directions and the boundary is not constrained by the Si(111)-7 × 7 unit cell edges. These clusters are randomly distributed on the terraces with 25 ± 5% (counted from the wide scan area) arranged along the step-edges (cf figures 4(a) and (b)). Within the type-2 cluster size range, a few clusters were also observed with well-defined sizes and shapes. Finally, type-3 clusters are large clusters with a base area in the range of 20 to a few hundred times the 7 × 7 unit cell area. The most significant feature of these clusters is that their boundaries are clearly separated by lines joining

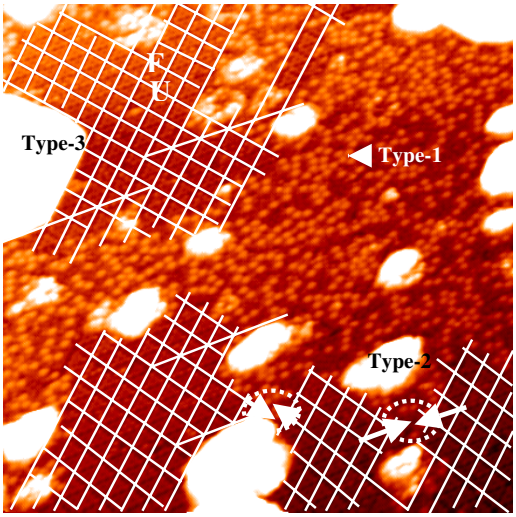

Figure 2. Filled-state STM image shows type-1, type-2 and type-3 clusters formed as Co is deposited on a Si(111)-(7 × 7) surface at RT and annealed first at 300 °C and second at 400 °C, both for 3 min: Co coverage ∼0.4 ML; $V_{tip} = +1.65$ V; scan size = 600 × 600 Å^2. The FH and UH of the Si(111)-(7 × 7) unit cell are marked separately by F and U. The dotted ellipse shows the area with dislocation.

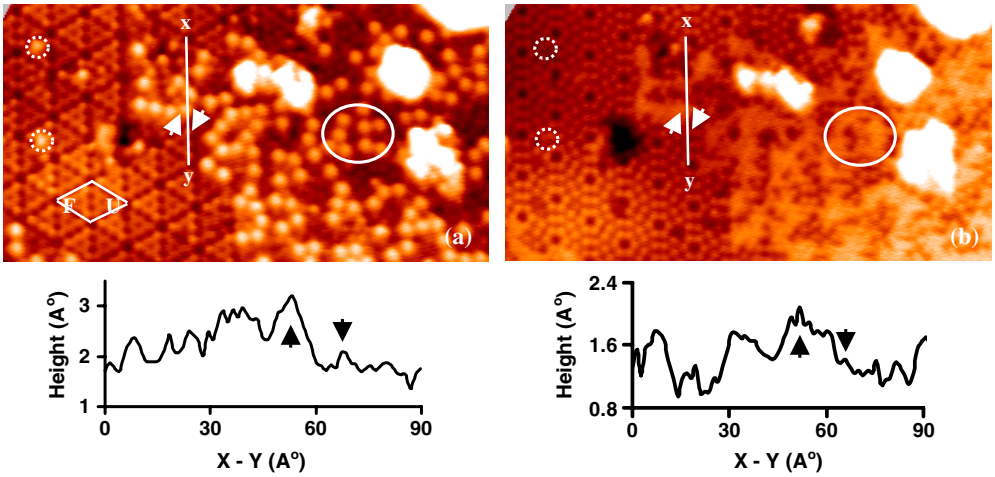

Figure 3. Filled-state (a) and empty-state (b) STM images of the same area and grown with the same conditions as the surface of figure 2: $V_{tip} = \pm 1.65$ V; scan size = 300 × 160 Å^2. The dotted circle shows the position of a silicide nucleus just below the surface: a white dot appears only in the filled-state image. The ellipse encloses a number of silicide nuclei that are on the surface. Here, we mention these as type-1 clusters. Individual spots are clearly visible in the filled-state only, but with a hazy appearance in the empty-state image. The line profile between two points XY shows the height difference of type-1 clusters in filled-state and empty-state images. The up and down arrows in the line profile indicate the positions of a type-1 cluster and a FH Si(111)-(7 × 7) Si corner adatom, respectively. The FH and UH of the Si(111)-(7 × 7) unit cell are marked separately as F and U.

the corner holes separating the faulted half (FH) and unfaulted half (UH) of the 7 × 7 unit cell (i.e. along the $\langle \bar{1}10 \rangle$ directions). The clusters are either approximately triangular or hexagonal

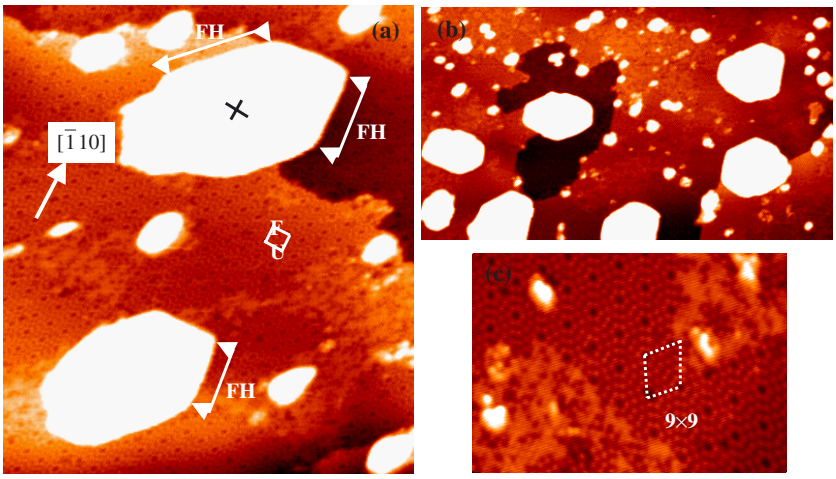

Figure 4. Empty-state STM image ($V_{tip} = -1.65$ V) of clusters grown with the same conditions as in figure 2. (a) Scan size 572× 652 Å^2, type-3 cluster edge bounded by FH has been marked by *FH*. The FH and UH of the Si(111)-(7 × 7) unit cell are marked separately as *F* and *U*. (b) Scan size 2000 × 1120 Å^2, showing an area where Si atoms have been consumed from a type-3 cluster-surrounded area. (c) A 9 × 9 reconstruction coexisted within the 7 × 7 matrix and near a type-2 cluster.

with atomically flat tops. They are randomly distributed on the terraces without any preference for the terrace edges.

We can obtain more information about type-1 clusters by analysing figures 3(a) and (b), the filled-state and empty-state STM images of the same area, and their corresponding line profiles. Type-1 clusters are clearly seen in the filled-state image as single isolated dots; however, in the empty-state image we only observe a hazy region in the 7 × 7 unit cells where the clusters were observed in the filled-state image. In the line profiles XY in figures 3(a) and (b), the up and down arrows indicate the positions of a type-1 cluster and a 7 × 7 FH corner Si adatom (which is the highest point of a Si(111)-7 × 7 reconstructed surface [16]) respectively. We determine the height of these type-1 clusters to be ∼1.1 ± 0.1 Å (0.7 ± 0.1 Å in the empty state). No such difference was observed between filled states and empty states for the other two types of clusters. The empty-state image in figure 3(b) allows us to clearly identify the smaller type-2 clusters by their bright appearance. The different topographic behavior of small type-2 clusters with respect to type-1 clusters is due to the coalescence of two or more type-1 clusters.

Figures 4(a)–(c) are taken from three other regions of the same substrate shown in figure 2 and show some additional features. In figure 4(a), the surface density of type-2 and type-1 clusters is low. Two straight edges of a type-3 cluster (marked by a cross) are bounded by the FH of Si(111)-7 × 7 and marked with arrows. It is also evident from the image that there is no depression around the type-3 clusters, and continuous Si(111)-7 × 7 terraces are clearly visible. We believe that Si consumption is from the terrace edges. Figure 4(b) shows a type-3 cluster surrounded by a one-bilayer-deep depression, and we postulate that it has consumed additional Si from that area in addition to atoms from terrace edges. Figure 4(c) shows an area between two type-3 clusters, and a Si(111)-9 × 9 unit cell near a type-2 cluster is highlighted.

4. Discussion

Understanding the kinetics of nucleation under different annealing conditions is important to fully explain Co silicide nucleation on Si(111)-(7 × 7). However in this study, we do not have

in situ real-time dynamical images. Nevertheless, by analysing these clusters and studying their evolution under varying annealing conditions, we postulate the mechanism of silicide growth. Bennett *et al* studied the Co/Si(111)-7 × 7 system, grown by both RT and high-temperature deposition, and proposed that, at very low coverages (∼0.016 ML) Co atoms diffuse to interstitial sites. When the concentration of interstitial cobalt is high enough, the so-called '*silicide nucleus*' is formed [9]. Comparing the filled-state and empty-state images in figures 3(a) and (b) respectively, we identify a cluster (marked by the dotted circle) that is clearly visible in the filled state but invisible in the empty state. We propose that such clusters exist below the surface as *silicide nuclei*, which are the precursor species that initiate silicide growth. We postulate that, above 300 °C, the *silicide nucleus* diffuses outward towards the surface, forming type-1 clusters. The ellipse shows a few type-1 clusters as bright dots (hazy appearance) in the filled state (empty state), as discussed earlier. These clusters grow at the first stage of silicide formation by breaking the local Si–Si bonds. The surface areas with local bond breaking reconstruct and regain their original 7 × 7 reconstruction above 300 °C. The formation temperature of Si(111)-7 × 7 is particularly dependent on the reaction pathways [17, 18]. We also observed Si(111)-9 × 9 unit cells near the type-2 clusters in figure 4(c), as well as Si(111)-5 × 5 unit cells elsewhere (not shown here).

STM studies of surface reconstruction, interface structure and growth kinetics of silicide islands grown by reactive epitaxy (RE) have been reported by Bennett *et al* [10, 19]; and SPE studies have been reported by Ilge *et al* [14] and Stalder *et al* [20]. Based on our STM observations, we explain the growth mechanism of different types of clusters grown by SPE. In regions with a high density of type-1 clusters (figure 2), we can still partially resolve the 7 × 7 structure. This leads us to postulate that, once type-1 clusters form, they diffuse on the surface without disrupting the 7 × 7 substrate. The growth and formation of type-2 clusters can be explained based on the Ostwald ripening (O-r) model [21, 22], whereby the larger clusters (e.g. type-2) grow at the expense of smaller clusters (e.g. type-1) due to the Gibbs–Thomson effect, i.e. by thermodynamically favouring the larger clusters. The O-r model is appropriate in the present case of SPE, where the clusters grow on a surface at zero deposition rates [21, 23]. We observe flat-tops and straight boundaries only for type-3 clusters, and these develop at the late stage of island formation. With prolonged annealing, either type-2 clusters out-diffuse adatoms which take part in the late stage coarsening (similar to classical O-r process) and eventually the flat-topped type-3 islands grow, or they consume additional material from the inter-island areas and convert to type-3.

The formation of a dimer-adatom-stacking-fault (DAS) [24, 25] family of reconstructions (i.e. metastable 5 × 5, 9 × 9 and stable 7 × 7) involves the activated surface transport of Si atoms [17, 18]. The observation of Si(111)-9 × 9 (figure 4(c)) and dislocations (figure 2, near type-2 clusters, shown by dotted ellipse), in addition to 7 × 7 in the inter-cluster areas, are common features in the SPE-grown Co/Si(111)-7 × 7 system. The formation of these different metastable phases is determined by the local concentration of Si adatoms [17, 18] and suggests the significant role of surface Si transport during silicide growth. On the other hand, dislocations are created due to the formation of different domains. Moreover, from the observation of the high density of type-1 clusters near the type-2 clusters (cf figures 2 and 3), we propose that the surface diffusion of Si atoms and type-1 clusters both play important roles in the formation of silicide islands.

Earlier reports show that silicide islands grown by RE at 320 °C are perfect triangular islands bounded by FH of 7 × 7 unit cells [10]. Stalder *et al* observed similar boundaries for silicide islands grown by SPE at 400 °C [26]. However, in figure 2 we observe two different faces bounded by UH and FH, respectively. Si on Si(111) homoepitaxy studies show that, although both triangular and hexagonal islands form, the hexagon being the equilibrium shape

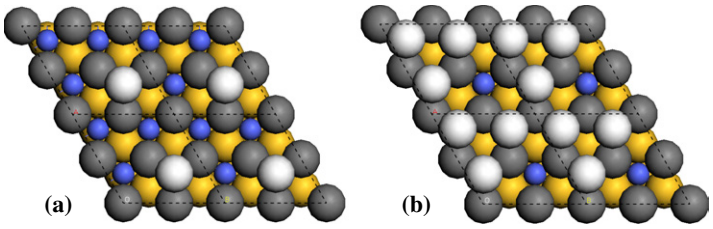

Figure 5. Top view of two possible $CoSi_2(111)$-2 × 2 structures terminated by two Si layers, (a) with one Si adatom per unit cell and (b) with three Si adatoms per unit cell. White, grey and yellow coloured spheres represent the first, second and third layers (counting from the top) of Si atoms, respectively. The Co atoms are denoted by blue spheres.

for which the energy of the island is minimized [27]. Moreover, in a stable configuration, the islands are always bounded by FH [10, 27]. We believe, at the straight-line edge of the type-3 cluster, a stacking fault is introduced (to match the FH boundary) which continues through the interface of the whole island, i.e. islands grow with so-called *B*-type orientation, as postulated in a previous study [26]. In this orientation, the epitaxial $CoSi_2$ phase is rotated 180° about the surface normal with respect to the substrate [12].

For bulk $CoSi_2(111)$, the Si–Co–Si triple-layer repeat unit in the z-direction is $5.36\ \text{Å}/\sqrt{3} = 3.097\ \text{Å}$ high. However, on multilayer or annealed $CoSi_2(111)$ films, different layer spacings have been observed, depending on different possible terminations of the top layers [28, 29]. The observed height of the 2 × 2 reconstructed island (marked by a cross) and grown at 300 °C in figure 1(a) is measured to be 22.6 ± 0.2 Å. The STM measured height of the islands observed in filled and empty-state images agree reasonably well and we consider this to be the true island height [19].

To understand the 2 × 2 corrugated silicide island surface reconstruction (figure 1(a)), we carried out first-principles total energy calculations. We simulated $CoSi_2(111)$ islands with vertical edges on Si(111). Based on the experimental observations, we constructed a lateral interface between the silicide and FH-Si(111)-7 × 7. Moreover, we considered a Si-rich surface which is terminated by two Si layers [26]. Pseudopotential DFT [30, 31] calculations were carried out using the Vienna *ab initio* simulation package (VASP) [32–34], which iteratively solves the Kohn–Sham equation in a plane-wave basis set. Here, the local-density approximation (LDA) [31] was employed for exchange and correlation energy, and Vanderbilt-type ultrasoft pseudopotentials [35] were used for all the elements. A cutoff energy of 250 eV was used in all calculations. The structure optimizations were converged to within 5 meV Å^{-1} for the total force per atom. After examining different Si-rich 2 × $2CoSi_2$ model structures on Si(111)-7 × 7, we deduced that two possible surface structures are consistent with observed island heights—structure '*a*' in figure 5(a) with one Si adatom per unit cell, and structure '*b*' in figure 5(b) with three Si adatoms per unit cell. As $CoSi_2(111)$ has one surface dangling Si bond in structure '*a*' and three in structure '*b*', structure '*a*' should be more stable then '*b*'. Hence, we propose an interface structure for a $CoSi_2(111)$ island on Si(111)-7 × 7 with a seven-fold Co coordinated interface and seven additional $CoSi_2$ layers on top of it, as shown in figure 6(a) in the $[1\bar{1}0]$ projection. The vertical dashed line in this figure shows the lateral interface along the island edges between $CoSi_2(111)$ and FH of Si(111)-7 × 7; and the island is of so-called *B-type* geometry. Previous experimental work also reported seven-fold Co coordination at the $CoSi_2(111)$/Si(111)-7 × 7 interface and *B-type* overlayer orientation [19, 36]. To simplify the calculation, we relaxed the left and right part of the vertical dotted line separately, and found that the height difference of the modelled $CoSi_2$ island and

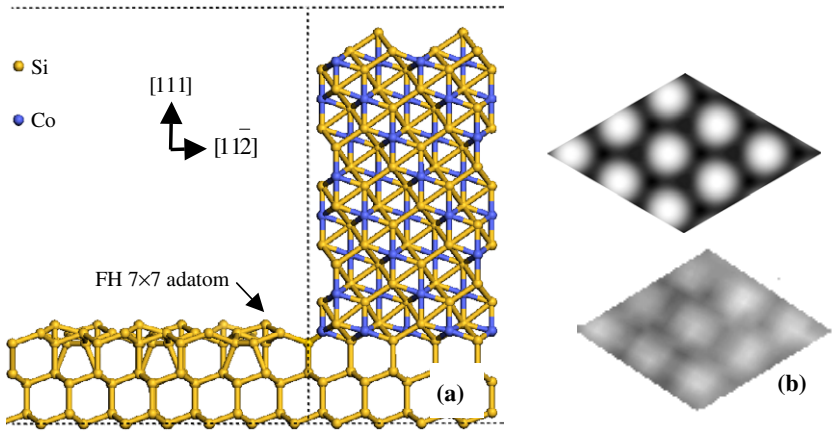

Figure 6. (a) Based on figure 5(a), the possible Si(111)/$CoSi_2$(111) interface structure in the [1$\bar{1}$0] projection, where the interface Co atom is seven-fold coordinated. Showing the *B-type* interface, the vertical dashed straight line is the interface between the $CoSi_2$(111) structure and the FH of Si(111)-7 × 7 unit cells. (b) Calculated and experimental (second row) empty-state STM images of the 2 × 2 reconstructed surface. The same bias voltage (1.8 V) as in the experimental image was considered for the present calculation.

the 7 × 7 adatom is 22.8 ± 0.1 Å. Considering the large height of the island (which limits the accuracy of the experimental height measurement), the calculated height agrees reasonably well with the STM measurement of 22.6 ± 0.2 Å.

Based on the 2 × 2 $CoSi_2$ structure of figure 5(a), we calculate the empty-state STM image of the reconstructed surface using the Tersoff–Hamann approach [37], as shown in figure 6(b). A bias voltage of 1.8 V was used for the present calculation. For comparison, we also present the experimental empty-state STM image of the 2 × 2 surface (scanned with the same bias voltage) at the same scale in the second row of figure 6(b). The calculated and experimental STM images agree well and further support our proposed model.

5. Conclusion

We have presented an STM study to explain the intermediate stages in Co silicide clusters and islands formation on Si(111)-(7 × 7). We identified type-1 clusters, which we propose as precursors to the formation of Co silicide. The observed metastable 9 × 9 phases and different domains on the surface, particularly near the type-2 clusters, suggest significant Si rearrangement during silicide island formation. We deduce the surface structure of the atom-resolved silicide islands and explain the interface structure of $CoSi_2$(111)/Si(111) with DFT calculations.

References

[1] Kläsges R, Carbone C, Eberhardt W, Pampuch C, Rader O, Kachel T and Gudat W 1997 *Phys. Rev.* B **56** 10801
[2] von Kanel H 1992 *Mater. Sci. Rep.* **8** 193
[3] Bennett P A and von Kanel H 1999 *J. Phys. D: Appl. Phys.* **32** R71
[4] Bennett P A, Copel M, Cahill D, Falta J and Tromp R M 1992 *Phys. Rev. Lett.* **69** 1224
[5] Alvarez J, de Parga A L V, Hinarejos J J, de la Figuera J, Michel E G, Ocal C and Miranda R 1993 *Phys. Rev.* B **47** 16048
[6] Sgarlata A, Szkutnik P D, Balzarotti A, Motta N and Rosei F 2003 *Appl. Phys. Lett.* **83** 4002

[7] Zuo J M and Li B Q 2002 *Phys. Rev. Lett.* **88** 255502
[8] Wawro A, Suto S, Czajka R and Kasuya A 2003 *Phys. Rev.* B **67** 195401
[9] Bennett P A, Cahill D G and Copel M 1994 *Phys. Rev. Lett.* **73** 452
[10] Bennett P A, Parikh S A and Cahill D G 1993 *J. Vac. Sci. Technol.* A **11** 1680
[11] Vrijmoeth J, Schins A G and van der Veen J F 1989 *Phys. Rev.* B **40** 3121
[12] Hellman F and Tung R T 1988 *Phys. Rev.* B **37** 10786
[13] Zilani M A K, Sun Y Y, Xu H, Liu L, Feng Y P, Wang X-S and Wee A T S 2005 *Phys. Rev.* B **72** 193402
[14] Ilge B, Palasantzas G, de Nijs J and Geerligs L J 1998 *Surf. Sci.* **414** 279
[15] Parikh S A, Lee M Y and Bennett P A 1995 *J. Vac. Sci. Technol.* A **13** 1589
[16] Hamers R J, Tromp R M and Demuth J E 1986 *Phys. Rev. Lett.* **56** 1972
[17] Kubby J A and Boland J J 1996 *Surf. Sci. Rep.* **26** 61
[18] Feenstra R M and Lutz M A 1990 *Phys. Rev.* B **42** 5391
[19] Bennett P A, Parikh S A, Lee M Y and Cahill D G 1994 *Surf. Sci.* **312** 377
[20] Stalder R, Sirringhaus H, Onda N and von Kanel H 1991 *Surf. Sci.* **258** 153
[21] Allmang M Z, Feldman L C, Nakahara S and Davidson B A 1989 *Phys. Rev.* B **39** 7848
[22] Allmang M Z, Feldman L C and Grabow M H 1992 *Surf. Sci. Rep.* **16** 377
[23] Zilani M A K, Xu H, Wang X-S and Wee A T S 2006 *Appl. Phys. Lett.* **88** 023121
[24] Takayanagi K, Tanishiro Y, Takahashi S and Takahashi M 1985 *Surf. Sci.* **164** 367
[25] Takayanagi K, Tanisbiro Y, Takahashi M and Takahashi S 1985 *J. Vac. Sci. Technol.* A **3** 1502
[26] Stalder R, Onda N, Sirringhaus H, von Kanel H and Lieuwma C W T B 1991 *J. Vac. Sci. Technol.* B **9** 2307
[27] Voigtlander B 2001 *Surf. Sci. Rep.* **43** 127
[28] Wu S C, Wang Z Q, Li Y S, Jona F and Marcus P M 1986 *Phys. Rev.* B **33** 2900
[29] Pirri C, Peruchetti J C, Bolmont D and Gewinner G 1986 *Phys. Rev.* B **33** 4108
[30] Hohenberg P and Kohn W 1964 *Phys. Rev.* **136** B864
[31] Kohn W and Sham L J 1965 *Phys. Rev.* **140** A1133
[32] Kresse G and Hafner J 1993 *Phys. Rev.* B **47** 558
[33] Kresse G and Furthmüller J 1996 *Phys. Rev.* B **54** 11169
[34] Kresse G and Furthmüller J 1996 *Comput. Mater. Sci.* **6** 15
[35] Vanderbilt D 1990 *Phys. Rev.* B **41** 7892
[36] Catana A, Schmid P E, Rieubland S, Levy F and Stadelmann P 1989 *J. Phys.: Condens. Matter* **1** 3999
[37] Tersoff J and Hamann D R 1985 *Phys. Rev.* B **31** 805